function in terms of the core and particle states. Another test of the core excitation picture could be accomplished by measuring the lifetimes of the low levels in Ca^{39} or K^{39}. The values in Table II should not be taken literally because of approximations used to compensate for a lack of experimental information about the transitions in Ca^{40}. Nevertheless, one expects at least $M2$ and $E1$ transition speeds to be considerably inhibited in the Ca^{39} or K^{39} level if core excitation is to be a reliable model. If higher $T=1$ core levels are mixing into the low Ca^{39} states, this inhibition will be considerably weaker and the usefulness of a core excitation picture should be questioned. This statement, however, assumes isotopic spin purity in the low levels of Ca^{40} and is at least consistent with the work of Erskine[27] for negative-parity levels, but the purity of the positive-parity levels has not been experimentally verified.

[27] J. R. Erskine, Phys. Rev. **149**, 854 (1966).

PHYSICAL REVIEW VOLUME 168, NUMBER 4 20 APRIL 1968

Production of Heavy Spallation Hypernuclei by 800-MeV/c K^- Mesons*†

A. LOU‡ AND D. T. GOODHEAD§
Physics Department, University of California, Los Angeles, California
(Received 20 October 1967)

The production of spallation hypernuclei is simulated by a Monte Carlo calculation. The results obtained from the present calculation are compared with those obtained experimentally from the interactions of 800-MeV/c K^- mesons with heavy nuclei (Ag or Br) in both $K2$ and $K5$ nuclear emulsions. The cascade stage was simulated in a very rough approximation; the evaporation stage was calculated in detail. The production features predicted from this calculation are in good agreement with those observed experimentally, except for the range distribution. The observed discrepancy is considered to be due to the rough approximation in the present computation in simulating the cascade stage. However, the present calculation indicates that the spallation model can still be regarded as a reasonable approximation to the production mechanism of heavy hypernuclei.

I. INTRODUCTION

IN order to study qualitatively the production features of short-range heavy hypernuclei based on the spallation model,[1,2] several calculations[3–5] have been carried out and the results compared with experimental observations. In terms of this model, the hypernucleus receives its momentum from the resultant of the momenta of the incident particle, the outgoing cascade particles, and the evaporated particles. For computational convenience, the initial interaction and the cascade process are assumed to give the nucleus a resultant momentum described by a fixed momentum $P_{\text{casc}}{}^b$ in the direction of the incident-beam particle and a randomly oriented momentum $P_{\text{casc}}{}^r$; these are not intended to correspond individually to separate physical processes. Then follows the evaporation of the excited nucleus, causing an additional momentum P_{evap}.

By neglecting the contribution from $P_{\text{casc}}{}^r$, Key *et al.*[3] concluded that P_{evap} was the main contributor to the final hypernuclear momentum. On the other hand, the results of Renard *et al.*[6] indicate that the total momentum imparted to the nucleus before the evaporation ($P_{\text{casc}}{}^b+P_{\text{casc}}{}^r$) may be the dominant factor (due to the magnitude of $P_{\text{casc}}{}^r$). Evans *et al.*,[4] in considering K^- captures at rest, assume that there is no forward component of the cascade momentum ($P_{\text{casc}}{}^b$) and that the only contribution to the final hypernuclear momentum is $P_{\text{casc}}{}^r$ and P_{evap}. Their results indicate that the contributions from both stages are of similar importance. Evans and Goodhead[5] have included all three stages in their calculation, and their results indicate that at high-incident K^- momenta of 6 BeV/c the contributions from P_{evap} are of little significance in the distribution of the final hypernuclear momentum.

In the present study, a Monte Carlo calculation was carried out to further investigate: (i) the validity of the spallation model in the production of hypernuclei; (ii) the significance of contributions from the three stages

* Work was partially supported by the National Science Foundation.
† Based on a Ph.D. thesis of one of us (AL).
‡ Present address: Physics Department, Augustana College, Sioux Falls, S. D.
§ Present address: Physics Department, Medical College of St. Bartholomew's Hospital, London, England.
[1] J. B. Harding, Phil. Mag. **42**, 63 (1951).
[2] B. D. Jones, B. Sanjeevaiah, J. Zakrzewski, M. Csejthey-Barth, J. B. Lagnaux, J. Sacton, M. J. Beniston, E. H. S. Burhop, and D. H. Davis, Phys. Rev. **127**, 236 (1962).
[3] A. W. Key, S. Lokanathan, and Y. Prakash, Nuovo Cimento **36**, 50 (1965).
[4] D. A. Evans, D. T. Goodhead, A. Z. M. Ismail, and Y. Prakash, Nuovo Cimento **39**, 785 (1965).
[5] D. A. Evans and D. T. Goodhead, Nucl. Phys. **B3**, 441 (1967).
[6] P. Renard, J. Sacton, and J. Zakrzewski, Nucl. Phys. **70**, 609 (1965).

to the final hypernuclear momenta; and (iii) the mass distribution of the hypernuclei which is relevant to the determinations of their binding energies (B_Λ) and the well depth of the Λ-hyperon in nuclear matter (D_Λ). The calculated results are compared with the experimental observations of 800-MeV/c K^- mesons.

II. EXPERIMENTAL DETAILS AND RESULTS

The data were obtained from two stacks of emulsions, viz., an Ilford $K2$ and an Ilford $K5$. The $K2$ emulsion stack was exposed to the 1.1-BeV/c K^- beam at the Berkeley Bevatron. Details of the beam design and experimental setup can be found in Ref. 7. The momentum of the degraded beam at the entrance edge of the target stack was approximately 800 MeV/c. One hundred pellicles of 600-μ-thick Ilford $K2$ nuclear emulsion of area 4 by 4 in. were used for exposure. The pellicles were divided into two stacks (stacks A and B). After exposure, the emulsions were mounted on glass holders, processed by the standard Bristol method,[8] and dried. The beam had a flux of about 5×10^5 K^- particles/cm^2, and it was approximately uniform over the entire stack. The ratios of K^--particle tracks in the emulsion to the background flux of lightly ionizing particles, viz., pions and muons, were approximately 1:0.15:0.85. Most of these background tracks are invisible, due to the insensitivity of the emulsion. The shrinkage factor for the $K2$ plates was measured as 2.35 from the known ranges of thorium stars.[9]

The $K5$ nuclear emulsion exposed to 800 MeV/c K^- beam was on loan to us through the kindness of Dr. W. H. Barkas and Dr. Norris Nickols. The grain density of the minimum ionizing tracks are found to be 28 grains/100 μm. The shrinkage factor is estimated to be 2.19.

The $K5$ and $K2$ plates were scanned under 375$\times$ magnification for interactions of high-energy K^- mesons. Each star was inspected under 1500$\times$ magnification for the presence of two centers or the interactions of secondary particles. The eyepiece reticle was aligned along each prong in turn, and the dip was extrapolated to the star center; if there was any doubt that all prongs were from the same center, the event was recorded as a possible double star and was reexamined later.

All double-centered events recorded during preliminary scanning were reexamined under 2500$\times$ magnification. Only events with two centers were accepted. Events for which the projected range of the connecting tracks between the two centers were less than 10 μm were classified as "double stars" (DS). Events for which it was possible to identify with certainty the origin of each prong as the primary or secondary center were labeled as "separable" (S) double stars, and those for which the origin of all prongs was not clear, but for which the existence of two centers was confirmed, were labeled as "nonseparable" events (NS).

All prongs from the primary center of the SDS events were classified as light (specific ionization $g^*<1.5$), grey ($1.5<g^*<10$), or black ($g^*>10$).

For $K2$ plates, the ranges and dip angles of DS connecting tracks were measured by the eyepiece reticle and fine-focus adjustments under 2500$\times$ magnification, while for $K5$ plates, the ranges and dip angles were measured under 1250$\times$ magnification with an eyepiece micrometer and fine-focus adjustment.

Two separate measurements were taken for both the range and dip by two different scanners. If the two measurements differed by more than 0.5 μm for either range measurements or depth measurements, a third measurement was carried out by a third observer. The average of the two closest values was chosen.

The forward/backward (F/B) ratios of (i) black prongs with respect to the hypernucleus (i.e., in the forward or backward hemisphere with respect to the hypernucleus), (ii) hypernucleus with respect to the incident beam, and (iii) black prongs with respect to the incident beam were all measured by the cross hairline in the eyepiece; an estimated reading accuracy of 0.5° was possible. Dip-angle measurements were made using the fine-focus adjustments calibrated to an accuracy of 0.5 μm.

The instrumental errors introduced in these measurements are usually less important than the errors common to all measurements in emulsion. The latter types of error have been fully investigated by various authors[10,11] and will not be discussed.

Figure 1 shows the range distributions of DS hypernuclei in the $K2$ and $K5$ emulsions. Due to the insensitivity of the $K2$ emulsions, this stack allows greater efficiency of detection in the short-range region (0–2 μm). It is assumed that all these DS events are due to hypernuclei and that any contamination due to other sources is insignificant.[3]

Table I shows the total yield of double stars (for different range groups of hypernuclei) from both $K2$ and $K5$ emulsions. The calculation of the production rate of heavy hypernuclei from these data is subject to the uncertainties in the contamination of π^- mesons in the incident beam and in the proportion of "cryptofragments" (i.e., hypernuclei of undetectable range).

Although there is certainly a scanning bias against

[7] R. B. Bell, R. W. Bland, M. G. Bowler, J. L. Brown, R. P. Ely, S. Y. Fung, G. Goldhaber, A. A. Hirata, J. A. Kadyk, J. Lowie, C. T. Murphy, J. S. Sahouria, V. H. Seeger, W. M. Smart, and G. H. Trilling, University of California Radiation Laboratory Report No. UCRL-11527 (unpublished).

[8] W. H. Barkas, *Nuclear Research Emulsions* (Academic Press Inc., New York, 1963).

[9] D. Garfinkle, M.S. thesis, University of California at Los Angeles, 1965 (unpublished).

[10] W. H. Barkas, F. M. Smith, and W. Birnbaum, Phys. Rev. **98**, 605 (1955).

[11] H. H. Heckman, B. L. Perkins, W. G. Simon, F. M. Smith, and W. H. Barkas, Phys. Rev. **117**, 544 (1960).

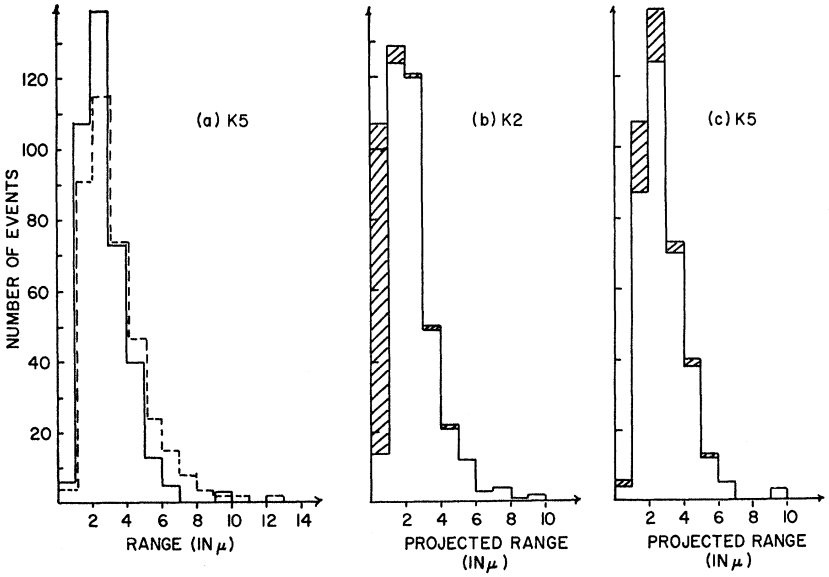

FIG. 1. Range distributions of DS hypernuclei (a) from $K5$ emulsion: - - - true range, —— projected range; (b) from $K2$ emulsion: (cross-hatched) NS (101 events), —— S (345 events); (c) from $K5$ emulsion, (cross-hatched) NS (43 events), —— S (344 events).

TABLE I. Total yield of beam stars and double stars from both $K2$ and $K5$ emulsions.

Emulsions	Total beam stars scanned	DS events classified S events (0–3)μ	(4–6)μ	(6–10)μ	NS events	Total DS events classified	Total DS events observed
$K2$	29 834	258	77	10	101	446	881
$K5$	11 689	215	120	8	41	385	385

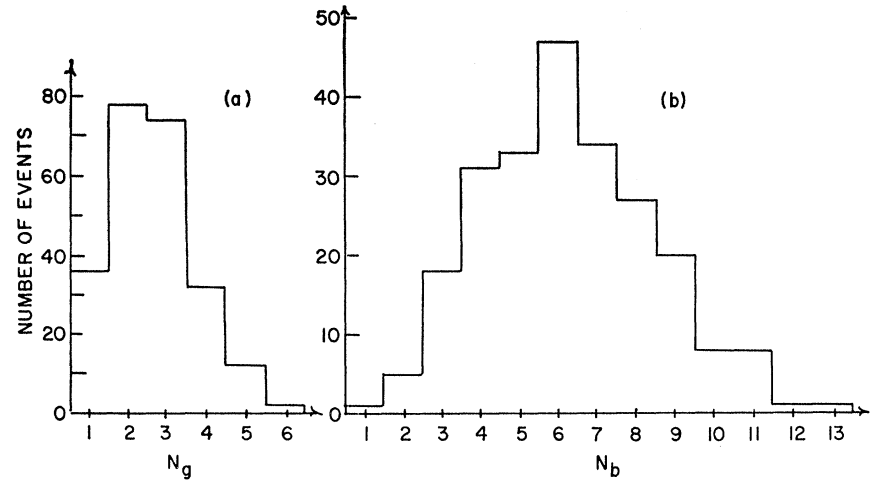

FIG. 2. (a) The N_g (number of grey prongs) distribution of the primary (production) center of 234 SDS from $K5$ emulsion. (b) The N_b (number of black prongs) distribution of the primary center of 234 SDS from $K5$ emulsion.

stars of small $N_h{}^+$ from both centers (including those with 0 or 1 prong in the decay center)[12] such a bias alone should not introduce too large an uncertainty in the production rate of heavy hypernuclei, since the presence of two centers should increase the detection efficiency. In addition, a random selection of K^- interaction stars from the original scan shows that 85% of the observed stars have $N_h \leq 8$; consequently, the observed low production rate of heavy hypernuclei from stars of $N_h \leq 8$ cannot be due primarily to scanning loss.

Figure 2 shows the N_b and N_g distributions of the primary centers of the separable double stars. From the

[12] This bias probably will be more appreciable in the results from $K2$ plates. ${}^+N_h$ is the number of "heavy" prongs for the star; it is the sum of the number of grey prongs (N_g, i.e., number of prongs of ionization $g^*>10$) and the number of black prongs (N_b, i.e., number of prongs of ionization $1.5<g^*<10$). The hypernuclear track is not included in either N_b or N_h.

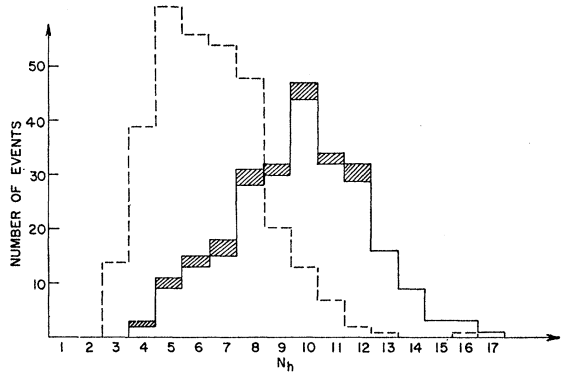

FIG. 3. Distributions of heavy prongs (N_h) from both centers of the 234 S (——), 21 NS cross-hatched DS, and a random sample (300) of K^- interactions (– – –).

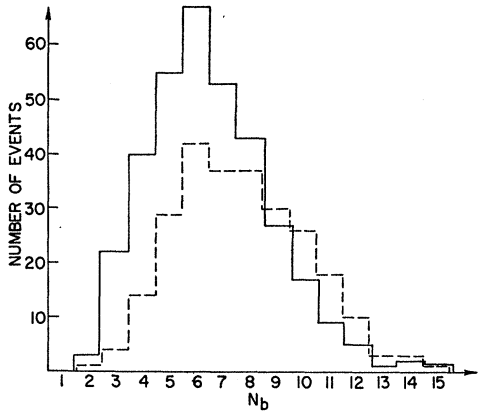

FIG. 4. Distributions of the black prongs (N_b) of the primary plus secondary centers of both S and NSDS from $K2$ (——) (345 events) and $K5$ (– – –) emulsions (255 events).

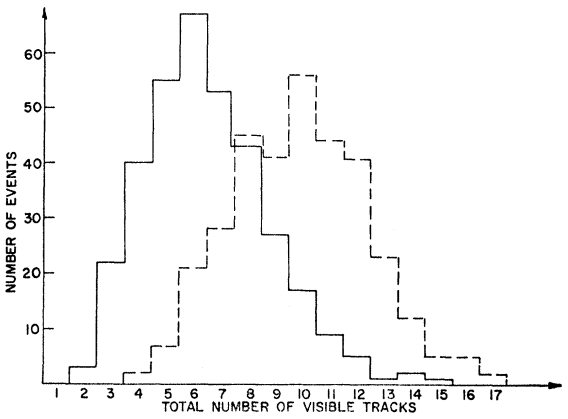

FIG. 5. Distributions of the total number of visible tracks (excluding the incident and hypernucleus tracks) of events found in both $K2$ —— (345 events) and $K5$ – – – (332 events).

data accumulated by various authors in this field, it is known that the mean $\bar{N}_b$ at the primary center (production center) increases as the momentum of the incident beam increases. This observation is explained in terms of the excitation energy of the evaporating nuclei. The mean excitation energy of the evaporating nuclei is increased and so is the $\bar{N}_b$ as the momentum of the incident beam increases.

Figure 3 shows the distributions of heavy prongs (N_h) from both centers of the SDS, the NSDS, and from a random sample of K^- interactions, respectively. It is seen that 83% of the S and 62% of the NSDS have $N_h \geq 8$. Since these prongs may be considered to be protons and heavier particles from the knock-on cascade and the evaporation stages of the interaction[3–6] it is clear that more than 80% of all the DS events originate from heavy nuclei of the emulsions.

In Fig. 4 are given the distributions of the black prongs (N_b) of the primary (production) and secondary (decay) centers of both S and NSDS events in both $K2$ and $K5$ emulsions. Figure 5 shows the distributions of the total number of visible tracks (excluding the incident and hypernucleus tracks) of events found in both $K2$ and $K5$ emulsions. The shape of the distribution is very similar, with the exception that there is a definite shift towards the lower number of visible tracks in K2 emulsions. This is probably due to the insensitivity of K2 emulsions.

The angular distributions of prongs from the interaction can give an indication of the kinematic processes involved in the primary interaction. According to the evaporation model, the F/B ratio of black prongs with respect to the incident beam is an indication of the center-of-mass velocity of the evaporating nucleus. (A similar F/B ratio is expected for the evaporated hypernuclei.) The observed data given in Table II are

TABLE II. F/B ratios of SDS of different ranges from $K5$ emulsions.

Hypernucleus range (μ)	0–3	3–6	6–10	0–10
F/B of hypernucleus with respect to K^-	3.12±0.93	3.44±1.06	1.63±1.03	3.10±0.62
No. of events	122	111	21	254
F/B of black prongs with respect to hypernucleus	0.70±0.08	0.43±0.06	0.56±0.14	0.57±0.05
No. of events	122	86	26	234
F/B of black prongs with respect to K^-	1.16±0.13	1.05±0.13	1.05±0.26	1.10±0.09
No. of events	122	86	26	234

TABLE III. F/B ratios of black prongs (N_b) with respect to hypernuclei for SDS of different black prong number from $K5$ emulsion.

N_b	0–4	5–6	7–8	9–12	0–12
F/B of black prongs with respect to hypernucleus	0.53±0.10	0.62±0.09	0.77±0.12	0.56±0.12	0.63±0.05
No. of events	88	81	47	18	234

consistent with evaporation from a very low velocity nucleus.

In terms of the spallation model, the F/B ratio of black prongs with respect to the hypernucleus is a measure of the contribution to the momentum of the spallation hypernucleus due to the evaporation prongs (P_{evap}). If P_{evap} were the sole contributor to the hypernuclear momentum, most of the evaporated particles should go backwards with respect to the hypernuclei and this effect should be comparatively more prominent for small N_b values. This tendency is not observed in the data shown on Table III. The fact that this F/B ratio does not decrease strongly as the N_b decreases indicates that the momentum contributed by the cascade particles $p_{\text{casc}}{}^r$ plays a large part in determining the magnitude and direction of the final momentum.

The significance of the F/B ratio of the hypernucleus with respect to the incident beam as shown in Table II is that it gives a clear indication whether the spallation process is a valid mechanism for the production of hypernuclei. If the heavy hypernuclei were actually produced as evaporation fragments instead of spallation products, the F/B ratio of the resultant hypernuclei to the incident beam should be close to 1. The shortness of the range distributions eliminates the possibilities of production of heavy hypernuclei by direct emission.

The correlation between the number of black prongs (N_b) and the number of grey prongs (N_g) as given in Table IV is not prominent in the present case; yet there exists a strong correlation between the two when the incident K^- beam has a momentum of 6 BeV/c.[5] The cascade and evaporation stages are not expected to be totally independent in the actual physical process but the above data suggests that this dependence is relatively less important at lower incident momenta. This was confirmed by preliminary Monte Carlo calculations for which correlation between N_b and N_g was ncluded.

TABLE IV. Correlation between number of grey prongs (N_g) and number of black prongs (N_b) of 234 SDS from $K5$ emulsion.

N_b \ N_g	0	1	2	3	4	5
0			1			
1	2	2	1			
2	1	10	5	1	1	
3	6	8	13	3	1	
4	3	9	12	7	2	
5	9	10	14	7	5	2
6	4	9	14	6	1	
7	4	14	5	2	2	
8	6	7	4	3		
9		3	2	3		
10	1	5	2			
11			1			
12		1				

III. MONTE CARLO CALCULATION

A model similar to that of Evans and Goodhead[5] is used in the present calculation. The main differences are in the use of the black-prong distribution, the variation of excitation energies, and the treatment of the evaporation process.

The observed mean number of black prongs ($\bar{N}_b$) is not used as an input parameter but the over-all shape of the N_b distribution is used as a constraint on the calculation. Dostrovsky *et al.*[13] have suggested that the N_b distribution from the evaporation of nuclei is narrower than a Poisson distribution if the nuclei all have the same initial excitation energy; however, the observed N_b distributions of DS events are rather wider than Poisson. This indicates that there is a spread of values of excitation energies of the evaporating nuclei. Consequently, a distribution of the initial excitation energies is used in the present calculation.

Instead of feeding in a fixed emission frequency for each evaporated particle, a detailed Monte Carlo calculation is carried out to simulate each step of the evaporation process. This results in more accurate mass and charge distributions of the residual hypernuclei and is relevant to the determination of B_Λ's and D_Λ from the decays of these hypernuclei.

Outline of Calculation

Each of the target nuclei Br^{80} and Ag^{108} are treated separately. For the sake of simplicity in computation, all the calculations are done in the rest frame of the nucleus.[14] A total of 4947 pseudoevents are generated.

Each pseudoevent commences with the cascade stage, which is immediately followed by the evaporation. For the cascade stage a method similar to that of Evans and Goodhead[5] is adopted, with $P_{\text{casc}}{}^b = 200$ MeV/c and $p_{\text{casc}}{}^r = 300$ MeV/c. The mass and charge of the target nucleus is reduced according to the number of nucleons

[13] I. Dostrovsky, P. Rabinowitz, and R. Bivins, Phys. Rev. **111**, 1659 (1958).

[14] In the calculations of Evans and Goodhead (Ref. 5) for hypernuclei produced by 6-BeV/c K^- mesons, center-of-mass corrections are applied whenever the velocity of the nucleus is greater than 10^{-4}, but it is found that these corrections have a negligible affect on the final results.

lost in the cascade stage. The observed grey-prong (N_g) distribution is used to determine the number of protons emitted by each event. From this, the number of neutrons is determined from a Poisson distribution of mean 1.5 times the N_g of that particular event. This proportion is arrived at from the average of the calculated data[15] and takes into account the excess of neutrons in the heavy nucleus. For the case of $N_g=0$, calculations are carried out for zero, one, or two neutrons, with equal weighting.

The evaporation stage follows a process similar to that of Dostrovsky *et al.*[16] The input data before the evaporation of each event include A and Z (of the residual nucleus after the cascade stage) and the excitation energy which may have a value of 100, 200, 300, 400, or 450 MeV. Results of different excitation energies are weighted so that the calculated N_b distribution matches that experimentally observed. The appropriate weighting factors are given in Table V.

The momentum impulses that the evaporated particles impart to the residual nucleus (P_{evap}) are combined with the momenta of the cascade stage ($P_{\text{casc}}{}^b$ and $p_{\text{casc}}{}^r$) and converted to the range of the heavy hypernucleus, using the range-momentum relations of Lou *et al.*[17]

The final results are obtained combining the separate distributions in the ratio of the geometric cross sections of Ag and Br nuclei in emulsions, viz., 1.2:1.[18] The uncertainties in this ratio are expected to be small.

Parameters Chosen

In the present calculation, all emission probabilities are relative to the emission probability of neutrons. In order for the calculation to be as close to the physical process as possible, even towards the end of the evaporation process, an approach similar to the modified one of Dostrovsky *et al.*[16] is employed in the calculation of emission probabilities of light particles (n, p, d, t, He^3, and α). However, in the calculations carried out by Dostrovsky *et al.*[16] a δ term was introduced to correct for the pairing and shell effect on the ground state of the residual nucleus, while in the present calculations, in order to save the computer memory core space, this δ term is included in the Q-value calculation; r_0 is taken to be 1.7 F.

An approximate form[19] is used in the calculations of the emission probabilities of multiply charged particles heavier than He^4 (He^6, Li^6, Be^7, Li^7, Li^8, and B^8). The ground states of B^8 and Li^8 are unstable against decay into two α particles,[20] but the B^8 and Li^8 tracks are observed experimentally (hammer tracks) and are therefore included in the calculation. Since the relative emission probabilities for all these multiply charged particles are similar, for computational convenience six times the emission probability of Be^7 is used to represent all these particles. The relative emission probabilities of the various charged particles are given in Table VI.

TABLE V. Weighting factors corresponding to initial excitation energies.

Weighting factor	Initial excitation energy (MeV)
0.5	100
1.0	200
0.7	300
0.1	400
0.1	450

The level-density parameter (a) is taken to be equal to $A/10$, since this value appears to give the best fit to experimental data.[21,22]

Wherever possible, the minimum separation energies (Q) of the particles evaporating from the nucleus are taken from the compilations of Wapstra,[23] based on experimental data. Where these are not available, the Q values of d, t, He^3, and Be^7 are calculated from the mass excesses computed by Seeger,[24] while the Q values of n, p, and α are taken directly from his table.

The effect of the Coulomb barrier corrections (V) on the ratios of the various particles emitted is discussed in detail by Dostrovsky *et al.*[13,16,21] The main effect of the barrier correction is to change the ratio of singly charged to doubly charged particles emitted in the evaporation process. For singly and doubly charged particles, Coulomb barrier corrections similar to those employed by Dostrovsky *et al.*[16] are used. For the particles of higher charge, the reduced Coulomb barrier as given by Lepekhin *et al.*[25]; $r_0=1.7$ F is used. The two

TABLE VI. Calculated emission frequencies of evaporated charged particles.

Particle	Calculated emission frequency
p	0.547±0.005
α	0.194±0.003
d	0.137±0.002
t	0.046±0.001
He^3	0.024±0.001
"Be^7"	0.053±0.001

[15] N. Metropolis, R. Bivins, M. Storm, J. M. Miller, G. Friedlander, and A. Turkevich, Phys. Rev. **110**, 204 (1958).
[16] I. Dostrovsky, Z. Fraenkel, and G. Friedlander, Phys. Rev. **116**, 683 (1959).
[17] A. Lou, L. R. Sandes, and D. J. Prowse, Nuovo Cimento **45B**, 214 (1966).
[18] M. M. Shapiro, in *Handbuch der Physik*, edited by S. Flügge (Springer-Verlag, Berlin, 1958), Chap. XLV, p. 342.
[19] J. Hudis and J. M. Miller, Phys. Rev. **112**, 1322 (1958).
[20] S. DeBenedetti, *Nuclear Interactions* (John Wiley & Sons, Inc., New York, 1966), Chap. II, p. 84.
[21] I. Dostrovsky, Z. Fraenkel, and L. Winsberg, Phys. Rev. **118**, 781 (1960).
[22] I. Dostrovsky, Z. Fraenkel, and P. Rabinowitz, Phys. Rev. **118**, 791 (1960).
[23] A. M. Wapstra, Physica **21**, 385 (1955).
[24] P. A. Seeger, Nucl. Phys. **25**, 1 (1961).
[25] F. G. Lepekhin, M. M. Makarov, and L. N. Tkach, Yadern. Fiz. **1**, 987 (1965) [English transl.: Soviet J. Nucl. Phys. **1**, 703 (1965)].

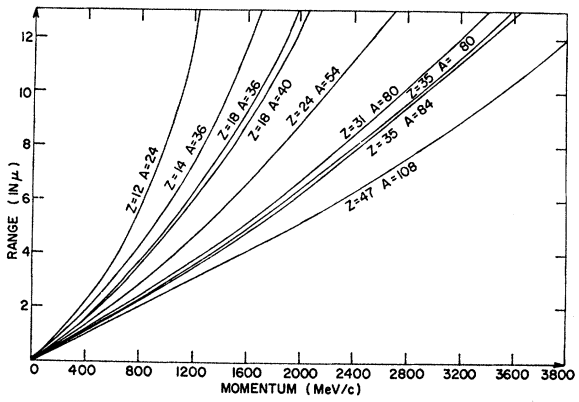

FIG. 6. Range-momentum curves for hypernuclei of different A and Z.

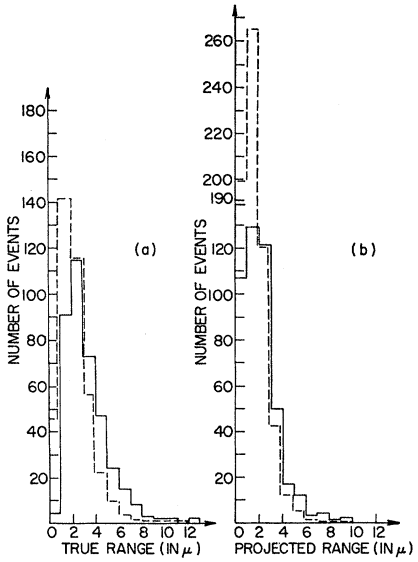

FIG. 7. Comparison of the calculated (– – –) and observed (——) range distributions normalized to the number of events of range (2–3) μm (a) from $K5$ emulsions, (b) from $K2$ emulsions.

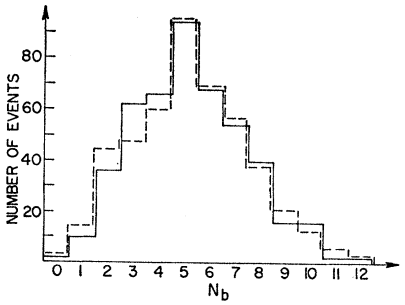

FIG. 8. N_b (number of black prongs) distribution obtained from 234 observed S (——) and 4947 calculated (– – –) hypernuclei. The calculated distribution is normalized to the number of observed events with five black prongs.

expressions for V are very similar, with the latter being dependent on the excitation energy of the nucleus before the emission of the particle.

The kinetic energies of the evaporated particles are calculated by a method similar to Dostrovsky *et al.*,[16] except that only one equation is used over the entire kinetic energy range. The two equations of Dostrovsky *et al.* do not lead to significant differences in the visible kinetic-energy spectra, so only their Eq. (18) is used.

Since the mean mass of heavy hypernuclei produced

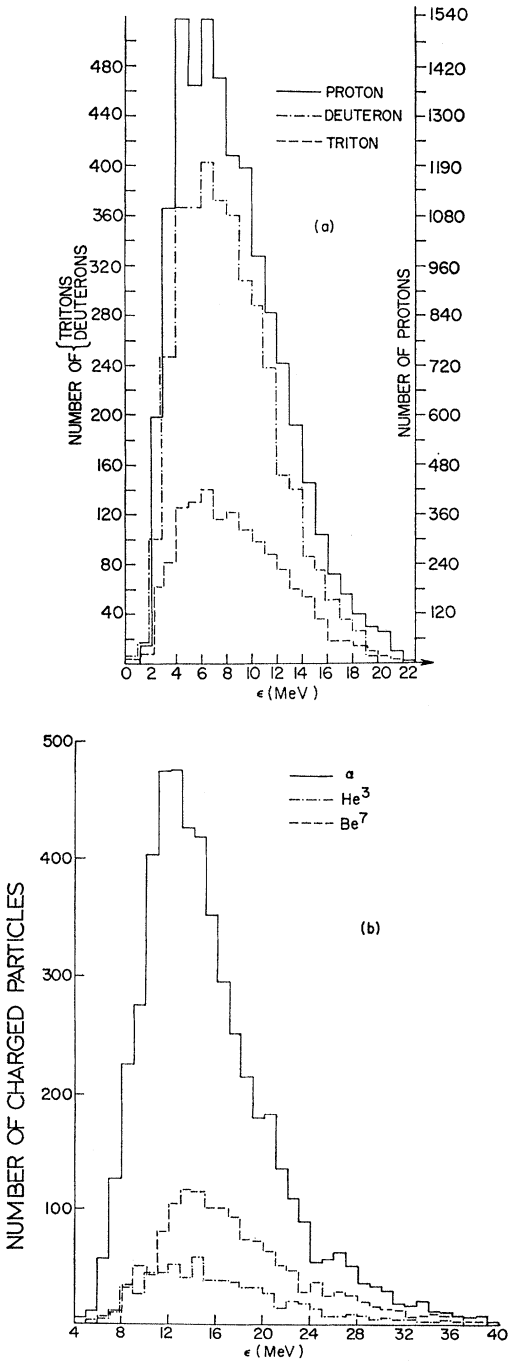

FIG. 9. Various spectra of visible kinetic energy (ϵ) distribution of (a) singly and (b) doubly and multiply charged particles.

TABLE VII. Observed and calculated F/B ratios of SDS of different ranges.

Hypernucleus range (μ)	F/B of hypernucleus with respect to K^-		F/B of black prongs with respect to hypernucleus		F/B of black prongs with respect to K^-	
	Observed	Calculated	Observed	Calculated	Observed	Calculated
0–3	3.12±0.93	2.50±0.001	0.70±0.08	0.70±0.01	1.16±0.13	1.17±0.02
3–6	3.44±1.06	2.95±0.29	0.43±0.06	0.45±0.02	1.05±0.13	1.04±0.04
6–10	1.63±1.03	5.10±2.33	0.56±0.14	0.35±0.06	1.05±0.26	1.05±0.16
0–10	3.10±0.62	2.61±0.001	0.57±0.05	0.63±0.07	1.10±0.09	1.14±0.02

by 800-MeV/c K^- mesons is about 75,[3,6] and the generalized range-energy relation of Heckman *et al.*[11] was tested experimentally only for particles up to A^{40}, the range-energy (range-momentum) relation derived by Lou *et al.*[17] is used to convert the resultant momentum of the spallation hypernuclei into range. The range-momentum conversion errors are estimated to be 20% for short ranges (<5 μm) and less for longer ranges. The calculated values of range versus momentum for several heavy ions, assuming that the entire C_z curve is universal,[26] are given in Fig. 6. It indicates clearly the extent of the effect of mass and charge on the range of a heavy hypernucleus with 1000-MeV/c resultant momentum (typical momentum imparted to the observed heavy hypernuclei, as indicated by Renard *et al.*[6]).

IV. RESULTS

A comparison of the calculated and observed F/B ratios of (i) black prongs with respect to beam, (ii) black prongs with respect to hypernucleus, and (iii) hypernucleus with respect to beam, is given in Tables VII and VIII. The good agreement is taken as an indication that the input values of $P_{\text{casc}}{}^b$ and $P_{\text{casc}}{}^r$ are reasonable.

The calculated range distribution of spallation hypernuclei is compared in Fig. 7 with the observed one. Since it was indicated by the studies of Bosgra and Hoogland[27] that a large observational loss is expected for hypernuclei of ranges less than 2 μm, the calculated range spectrum is normalized to the number of hypernuclei with ranges of 2–3 μm, where the scanning losses are expected to be small. However, there is a disagree-

TABLE VIII. Observed and calculated F/B ratios of black prongs (N_b) with respect to hypernuclei for SDS of different black prong number.

N_b	(F/B) ratio of black prongs with respect to hypernucleus	
	Observed	Calculated
0–4	0.53±0.10	0.58±0.02
5–6	0.62±0.09	0.62±0.01
7–8	0.77±0.12	0.66±0.02
9–12	0.56±0.12	0.67±0.03
0–12	0.63±0.05	0.63±0.01

[26] For values of $137\beta/Z \leq 0.07$, a second-order polynomial obtained by Lou *et al.* (Ref. 17) is used as an interpolating function between (0,0) and $137\beta/Z=0.07$. For values of $137\beta/Z \geq 0.55$, a least-squares fit to the mean values of N^{14}, O^{16}, and Ne^{20} obtained from the range-energy data of Heckman *et al.* (Ref. 11) is used. For intermediate values further experimental data are desirable in order to test that the entire C_z-versus-$137\beta/Z$ curve is universal.

[27] S. J. Bosgra and W. Hoogland, Phys. Letters **9**, 345 (1964).

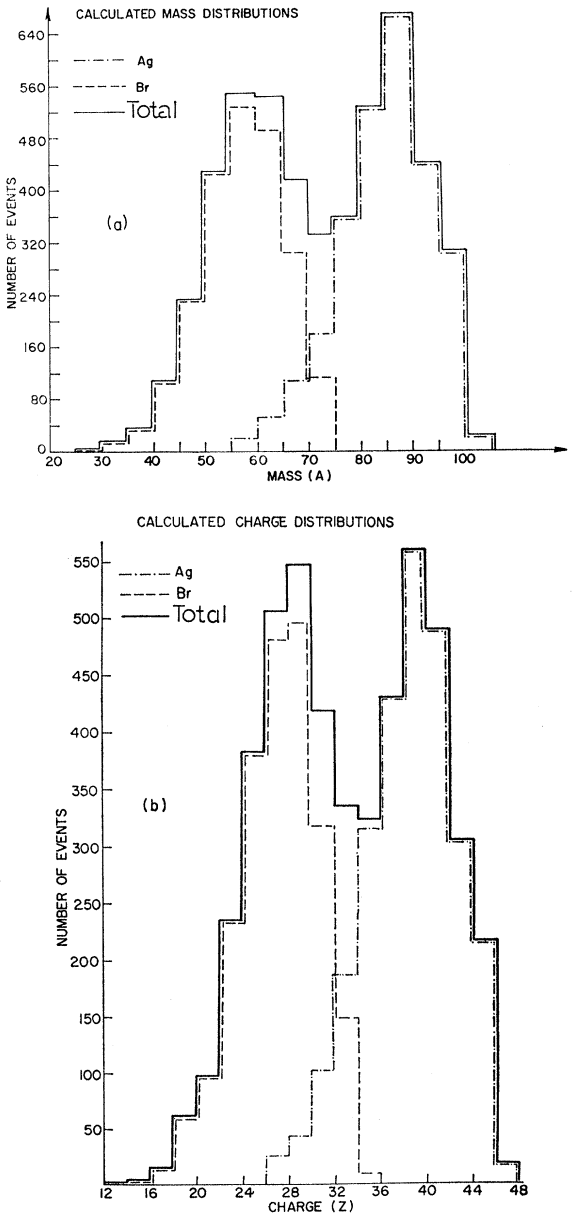

FIG. 10. The mass and charge distribution of the spallation hypernuclei: (a) mass (A), (b) charge (Z).

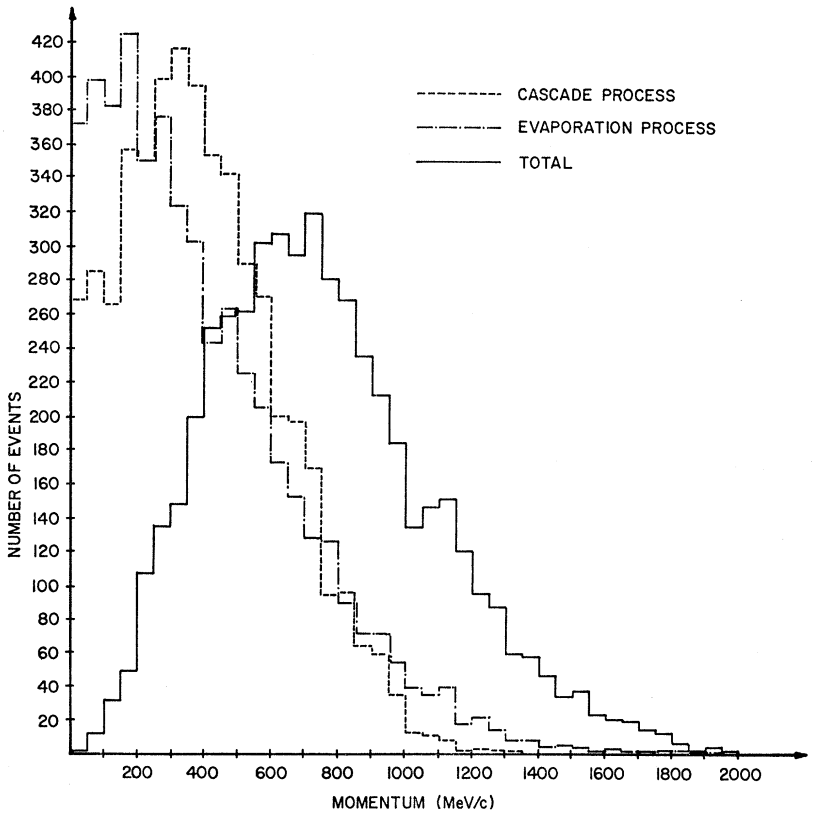

FIG. 11. The distribution of the calculated resultant momentum imparted to the hypernucleus. Also shown are the individual distributions of the contributions of the cascade (– – –) and the evaporation (— — — —) processes; the values shown are those of the components of $p_{\text{casc}}{}^{r}+p_{\text{casc}}{}^{b}$ (– – –) and of P_{evap} (— — — —) in the direction of the resultant momentum of the hypernucleus.

ment between the calculated and observed range distribution for the hypernuclei of range greater than 3 μm. The calculated spectrum has a noticeably sharper cutoff.

The N_b distribution obtained from the calculation and that observed experimentally are shown in Fig. 8. The weightings of the initial excitation energies of the calculated events were chosen to give reasonable agreement between these two distributions.

Figure 9 gives the various spectra of visible kinetic-energy distributions of singly, doubly, and multiply charged particles. The cutoff of each spectrum confirms the validity of the assumption that the observed prongs of $g^{*}>10$ are produced during the evaporation process. It may be added that a general flattening of the spectra occurs for smaller values of a and therefore experimental spectra may be able to provide a check on the correctness of a chosen for the computation.

V. DISCUSSION

It is seen that the calculated range distribution has a sharper long-range cutoff than the observed distribution (Fig. 7) and this becomes more pronounced if the contribution due to the cascade momentum is neglected. Furthermore, as discussed previously, the observed F/B ratios of black prongs with respect to hypernuclei require that $p_{\text{casc}}{}^{r}$ plays a major role. This discrepancy in observed and calculated ranges could be due to the fact that too simplified a model is used in the calculation of the cascade process. That the cascade process plays a dominant role in the spallation process is demonstrated by the F/B ratio of black prongs with respect to hypernuclei. At higher incident beam momenta (e.g., 6 BeV/c)[5] the cascade process clearly is highly correlated to the evaporation as is shown by the correlation of N_g and N_b at these momenta.

The calculated mass and charge distribution of the spallation hypernuclei are presented in Fig. 10. The double peak is due to the combination of contributions from two different target nuclei (Ag and Br). It should be noted that some hypernuclei have masses as low as $A\sim 15$. The residual hypernuclei are proton rich. The fact that the cascade process was only roughly simulated should not cause much error in the mass and charge distributions which are determined primarily by the evaporation.

Figure 11 shows the calculated distribution of the resultant momentum imparted to the heavy hypernuclei during the cascade and evaporation stages. The shape of the spectrum from Ag does not differ much from that from Br. The distribution peaks at about 700 MeV/c and has a tail extending to about 2000 MeV/c. This is in agreement with the fact that the cascade momentum (i.e., the total momentum imparted to the nucleus before evaporation) obtained by Renard *et al.*[6]

from a completely different approach extends up to about 1800 MeV/c.

The calculated distribution of the binding energy of the least-bound proton in the heavy hypernuclei is given in Fig. 12. This distribution is obtained from each individual set of A and Z of the residual hypernuclei obtained in the present Monte Carlo calculation by applying Seeger's semiempirical mass formula.[24] It is demonstrated from this distribution that most of the spallation residues in which the Λ remains trapped may not be on the stability line; therefore, the binding energy of the least-bound proton is quite large. Since the error introduced in estimating the binding energy of the least-bound proton is the major source of error in the estimation of B_Λ,[28] there is doubt regarding the real significance of the "π-r" decays in obtaining the true B_Λ's.

The results of the Monte Carlo calculation could be used as follows to estimate D_Λ (the well depth of the Λ-hyperon in nuclear matter) from the observed π-p-r events: By comparing the observed event with all the calculated "pseudoevents" of identical N_b and N_g at the primary center and of similar range,[29] it is possible to estimate the probable A and Z values of that observed hypernucleus. This procedure should be preferred over a more direct estimate of the exact A of each event because of the difficulties in experimentally identifying all the charged particles and estimating the number of neutrons. From the calculated distribution of probable A and Z values as deduced above and the observed B_Λ associated with each "π-p-r" event, the well depth D_Λ can be approximated. The calculated results from the lower A and Z values should be slightly more favored since the exclusion principle favors mesonic decays from lower A hypernuclei.

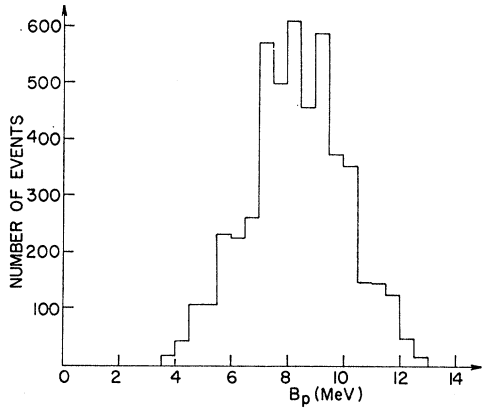

FIG. 12. The distribution of the binding energy of the least-bound proton in the heavy hypernuclei.

ACKNOWLEDGMENTS

The first author wishes to express her gratitude to her sponsor, Dr. D. J. Prowse, for suggesting the problem and in particular, for his invaluable assistance in the initial phase of this work. The completion of this work was possible only through his continuous encouragement and invaluable guidance. The emulsion laboratory of the physics department of U.C.L.A. is thanked for providing the facilities during the course of the present investigation. Dr. Norris Nickols is thanked for the loan of Dr. Walter H. Barkas's $K5$ emulsion stack. The help contributed by the scanning team of the U.C.L.A. emulsion group is gratefully acknowledged. The Lawrence Radiation Laboratory of Berkeley is thanked for the facilities provided during the exposure of the $K2$ emulsion stack.

[28] In the case of "π-r" decays, $B_\Lambda = 37.6 + 8 -$ (visible energy released by π). Since both Q_Λ and the visible energy released by the π can be determined fairly accurately ($\pm 2\%$), a 2-MeV shift in B_p would cause an approximately 10% shift in B_Λ.

[29] The observed range (R) and the calculated range of a pseudo-event (R_c) are treated as similar if $0.7R < R_c < 1.5R$.